Radiation Protection Dosimetry (2006), Vol. 119, No. 1–4, pp. 111–114
doi:10.1093/rpd/nci584 Advance Access published on March 31, 2006

THEORETICAL MODELLING OF EXPERIMENTAL DIAGNOSTIC PROCEDURES EMPLOYED DURING PRE-DOSE DOSIMETRY OF QUARTZ

Vasilis Pagonis[1,*], Reuven Chen[2] and George Kitis[3]
[1]Physics Department, McDaniel College, Westminster, MD 21158, USA
[2]School of Physics and Astronomy, Raymond and Beverley Sackler Faculty of Exact Sciences, Tel-Aviv University, Tel-Aviv 69978, Israel
[3]Aristotle University of Thessaloniki, Nuclear Physics Laboratory, 540 06 Thessaloniki, Greece

The pre-dose technique in thermoluminescence (TL) is used for dating archaeological ceramics and for accident dosimetry. During routine applications of this technique, the sensitisation of the quartz samples is measured as a function of the annealing temperature, yielding the so-called thermal activation characteristic (TAC). The measurement of multiple TACs and the study of the effect of UV-radiation on the TL sensitivity of quartz are important analytical and diagnostic tools. In this paper, it is shown that a modified Zimmerman model for quartz can successfully model the experimental steps undertaken during a measurement of multiple TACs.

INTRODUCTION

The theoretical basis of the well-established pre-dose technique is the original model introduced by Zimmerman[(1)]. Chen and Leung[(2)] developed a mathematical form of the Zimmerman model, which successfully explained several important physical phenomena associated with the thermoluminescence (TL) of quartz.

Thermal activation characteristics (TACs) of quartz samples are an important analytical and diagnostic tool used routinely during TL predose dating of quartz and during retrospective dosimetry. In particular, TACs are very useful in (1) finding the temperature of maximum sensitivity, which is used during the predose technique, and (2) in identifying partially activated samples by comparing the shapes of multiple TACs[(3)].

The TACs of quartz are measured experimentally by heating a single aliquot of the sample to a series of increasing temperatures typically from 150 to 700°C, and by measuring the response to a small test dose after each heating stage. The test dose is typically in the range of 10 mGy.

Recently, Chen and Pagonis[(4)] simulated the experimental measurement of TACs in quartz by using the modified four-level Zimmerman model of Chen and Leung[(2)]. These authors showed that the exact shape of TACs depends on the type of quartz studied and on the thermal and radiation history of the sample. The simulation explained the general shape of TACs and the decrease in sensitisation known as thermal deactivation[(3,5,6)]. The measurement of multiple TACs on the same sample (aliquot) is an important diagnostic and analytical tool, and is routinely applied during application of the pre-dose technique[(7,8)]. In a typical measurement of multiple TACs a laboratory dose is given to the sample after the measurement of the first TAC is completed, and a new second TAC is measured using the same experimental protocol. By comparing the shapes of the first and second TAC, it is possible to identify samples that may have been partially activated during the history of the material.

Haskell and Bailiff[(8)] and Bailiff and Haskell[(9)] examined in detail the temperature shifts in the thermal activation curves of multiple TACs, and found that the second TAC was shifted towards lower temperatures exhibiting the 'early activation' phenomenon. These authors concluded that these shifts to lower temperatures were not due to ambient activation but rather were due to the thermal and irradiation history of the samples.

It is noted that the published data on multiple TAC measurements are of an empirical nature and that no mathematical description of these phenomena has been published previously.

DESCRIPTION OF THE MULTIPLE TAC SIMULATION

The energy scheme used by Chen and Leung[(2)] is a modification of the original Zimmerman model[(1)], and its details have been given previously elsewhere[(2,4,10)]. The notation used in this paper is identical to the one used in Chen and Leung[(2)].

*Corresponding author: vpagonis@mcdaniel.edu

Chen and Pagonis[4] showed that the model can simulate the series of experimental stages during a typical single TAC measurement as follows:

(1) *Natural irradiation stage*: During this stage the sample is assumed to be irradiated for time, t_1, in nature. A relaxation time of 60 s is simulated at this stage, at the end of which the concentrations n_c and n_v relax to zero.
(2) *Heating stage*: The sample is heated from room temperature to an activation temperature of 300°C with a heating rate of +5°C s^{-1}. This heating stage causes some of the holes in the reservoir R to be released and to be captured in the luminescent centre, L. This stage is followed by a cooling down period room temperature with a constant cooling rate of 5°C s^{-1}.
(3) *Irradiation with test dose*: The sample is irradiated for a time period $t = 1$ s with a dose rate x, resulting in a delivered dose of $D = x \cdot t =$ 5.108 cm^{-3}. A relaxation time of 60 s follows this irradiation stage.
(4) *Measurement of '110°C' TL glow peak*: The TL glow peak is measured by heating to 150°C. The maximum of the TL peak (TL_{max}) is recorded. This stage is followed by a cooling down period to room temperature with a constant cooling rate of 5°C s^{-1}. The concentrations of n_s, n_t, m, n_c, n_v and n_r at the end of this cooling down period are used as the initial values for repeating Step 1 using a slightly higher annealing temperature.
(5) The series of Steps 1–4 above is repeated several times using a slightly higher activation temperature each time, in increments of 50°C, up to a maximum temperature of 600°C.

The simulation presented in this paper extends the above procedure, by simulating the measurement of a second TAC on the same aliquot, as follows:

(6) *Laboratory irradiation stage*: At the end of the first TAC measurement, the sample is irradiated again for a time, t_2, at room temperature, to simulate irradiation of the sample between TACs in the laboratory. A relaxation period of 60 s is again incorporated.
(7) The traps are cleared by heating the sample to 150°C. A cooling down period to room temperature is again simulated.
(8) Steps 1–4 above are repeated for a series of increasing annealing temperatures, and the second TAC is obtained.

The result of the simulation is the multiple TAC graphs shown in Figure 1.

It is noted that at the end of the laboratory irradiation stage (step 6) as described above, the sample may exhibit a markedly changed sensitivity to the test dose. This change can be either an increase in sensitivity termed 'radiation sensitisation' or a decrease in sensitivity termed 'radiation quenching'[3,5].

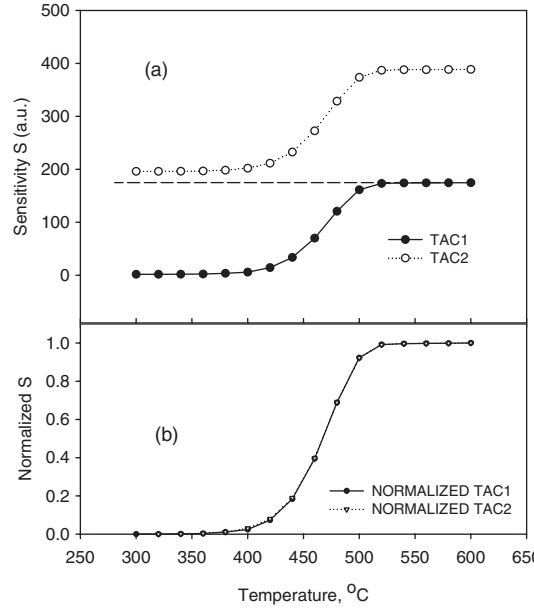

Figure 1. (a) The first and second TACs calculated for the irradiation times $t_1 = 1000$ s and $t_2 = 1000$ s. (b) The normalised TACs are found to be identical, and sensitisation is taking place between the two TACs.

NUMERICAL RESULTS AND DISCUSSION

Multiple TACs: the case of radiation sensitisation

Figure 1a shows the result of simulating the first and second TAC using the same parameters as in Pagonis *et al.*[10]. At the start of the simulation the traps and recombination centres are assumed to be empty. The natural irradiation time is taken to be $t_1 = 1000$ s, whereas the laboratory beta irradiation time is taken as $t_2 = 1000$ s. Figure 1b shows the normalised TACs, which are seen to be identical; hence, no change in the shape of the TAC takes place between the first and second TAC cycle.

Figure 1a also shows that radiation sensitisation takes place between the two TACs, as indicated by the location of the dashed line, which serves as a guide to the eye.

Multiple TACs: the case of radiation quenching

By introducing the slightly different values of the capture probability coefficients $A_m = 0.5 \times 10^{-11}$ cm^3 s^{-1} and $A_s = 10^{-12}$ cm^3 s^{-1}, the quartz sample shows a decreased sensitivity after the laboratory irradiation stage and heating. This phenomenon is known as

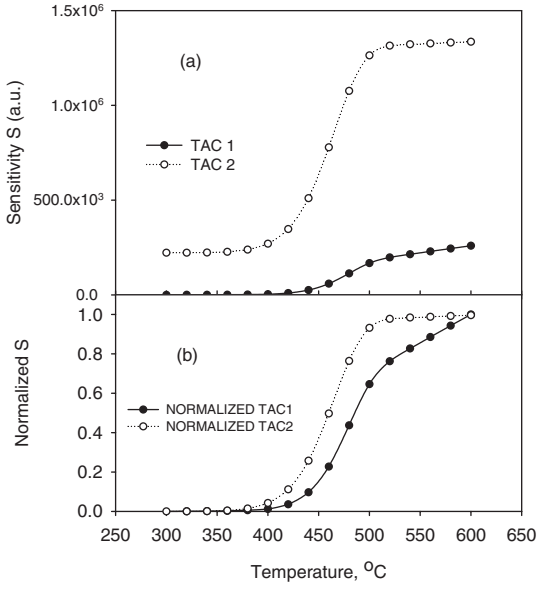

Figure 2. (a) The same as in Figure 1, with the irradiation times $t_1 = 1$ s and $t_2 = 100$ s. (b) The normalised TACs are no longer identical.

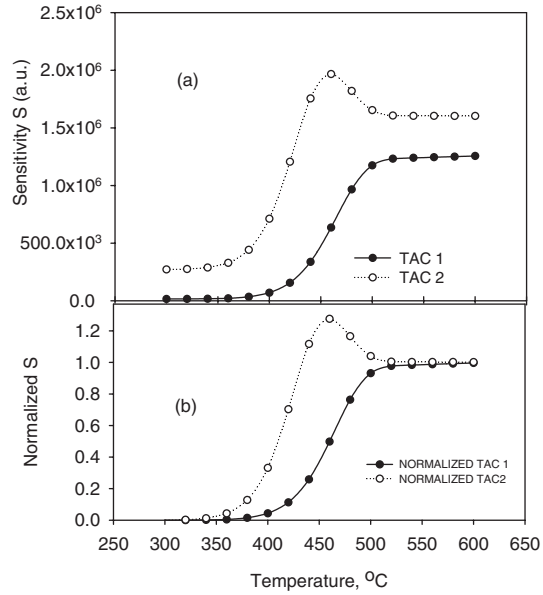

Figure 3. (a) The same as in Figure 2, with the irradiation times $t_1 = 100$ s and $t_2 = 1000$ s. (b) The first TAC shows no deactivation effects, whereas the second TAC shows the characteristic deactivation behaviour.

radiation quenching. The normalised TACs in the case of radiation quenching were also found to be practically identical.

Multiple TACs: changes in the shape of TACs due to the sample's thermal and irradiation history.

Figure 2a shows the result of measuring the first and second TAC using the same kinetic parameters, and with the natural irradiation time taken as $t_1 = 1$ s, whereas the laboratory beta irradiation time is taken as $t_2 = 100$ s. Figure 2b shows that the shapes of the normalised TACs are now drastically different. The first TAC shows a rather continuous increase in the sensitivity with the temperature, whereas the second TAC reaches a plateau $\sim$520°C.

These results from the model are very similar to the unusual results obtained experimentally by Haskell and Bailiff[8] (Figure 1) and to the results of Bailiff[11] (Figure 1). These authors found that there is a significant difference between the normalised first and second TACs of a very similar form to that shown in the calculations of Figure 2b.

Multiple TACs: changes in the deactivation region of TACs

Figure 3 shows the results of running the simulation using the values of natural irradiation time $t_1 = 100$ s, and the laboratory irradiation time $t_2 = 1000$ s and using the same kinetic parameters. The data in Figure 3 show that it is possible for the first TAC to show no deactivation effects, whereas the second TAC shows the characteristic deactivation behaviour at temperatures above 470°C. Similar results were obtained previously experimentally by Aitken[12] (shown in their Figure 2), but no satisfactory explanation was provided previously for this effect. Within the current model, the observed differences in the shape of the first and second TAC are owing to the different doses received by the sample in nature and in the laboratory.

SIMULATION OF THE UV-REVERSAL EFFECT

The UV-reversal effect consists of the following: a quartz sample is sensitised to ionising radiation by heating to a high-annealing temperature, e.g. 500°C. This annealing sensitises the sample by transferring holes from the reservoir, R, to the luminescence centre, L (the pre-dose effect).

The sample is now illuminated with UV-light, which results in a reduced sensitivity to ionising irradiation. The empirical explanation of the sensitivity reversal is that the UV-exposure ejects holes out of the luminescence centre, L. In reality, the UV excites electrons out of the valence band, and these electrons are recombined with holes at the luminescence centre, L, hence, reducing the concentration of holes in L[1].

Previous experimental studies of this UV-reversal have shown that the sensitivity can be reduced commonly by as much as 90–95% of its original value[2,3].

The differential equations in the Chen and Leung[2] model were changed as follows, so that the model describes the UV-reversal effect:

$$\frac{dm}{dt} = -R \cdot m + A_l * n_v * (M - m) \quad (1)$$

$$\frac{dn_v}{dt} = +R \cdot m - A_l * n_v * (M - m) - A_r * n_v * (N_r - n_r) \quad (2)$$

$$\frac{dn_r}{dt} = +A_r * n_v * (N_r - n_r) \quad (3)$$

The term $A_l * n_v * (M - m)$ in Equation 1 expresses the capturing of holes into L from the valence band.

The term $-A_r * n_v * (N_r - n_r)$ in Equation 2 expresses the capturing of holes from the valence band into the reservoir R.

The equations describing the traffic of electrons in the trap T and the competitor S during the heating stage are left unchanged, since the electrons are not involved in the UV-irradiation process.

Figure 4 shows the result of solving the above differential equations for the following stages:

(1) An initial value of the concentration of competitors $n_s(0) = 10^{12}$ cm^{-3} is assumed, as well as $n_t(0) = n_c(0) = n_v(0) = 0$. The concentration of holes in the luminescence centre, L, is varied from $m(0) = 0$ (all holes are in the reservoir), to $m(0) = 10^{12}$ cm^{-3} (no holes are in the reservoir). In all cases the concentration of holes in the reservoir is calculated using $n_r(0) = n_s(0) - m(0)$. All the other parameters are left the same.
(2) The initial TL sensitivity to a test dose is measured.
(3) The sample is UV-irradiated at room temperature for a certain length of time (t_{uv}).
(4) The new TL sensitivity is measured by administering the same test dose.
(5) The process (a)–(d) is repeated for a longer UV-irradiation time.

Figure 4 shows that as the irradiation times get longer, the TL sensitivity is reduced down to a 'residual value', which depends on the initial concentration $m(0)$.

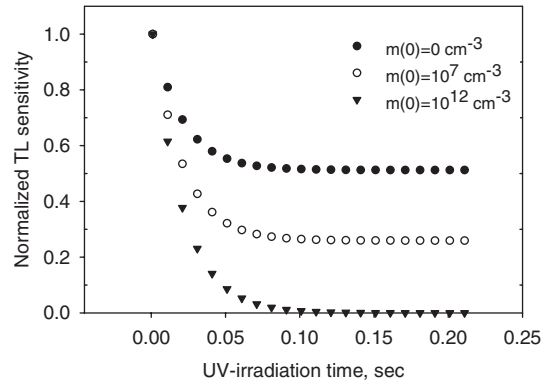

Figure 4. Simulation of the UV-reversal effect for various initial concentrations of holes in the reservoir $n_r(0)$.

CONCLUSIONS

The results presented in this paper show that the shape and behaviour of multiple TACs depend critically on the doses received by the sample in nature and in the laboratory. It is also shown that the model provides for a quantitative description of the well-known phenomena of radiation quenching and radiation sensitisation.

REFERENCES

1. Zimmerman, J. *The radiation induced increase of the 100° C TL sensitivity of fired quartz*. J. Phys. C Solid State Phys. **4**, 3265–3276 (1971).
2. Chen, R. and Leung, P. L. *Modelling the pre-dose effect in thermoluminescence*. Radiat. Prot. Dosim. **84**, 43–46 (1999).
3. Aitken, M. J. *Thermoluminescence Dating* (London: Academic Press) (1985).
4. Chen, R. and Pagonis, V. *Modelling thermal activation characteristics of the sensitization of thermoluminescence in quartz*. J. Phys. D Appl. Phys. **37**, 159–164 (2004).
5. Fleming, S. J. *Thermoluminescence Techniques In Archaeology* (Oxford: Clarendon Press) (1979).
6. Bailiff, I. K. *The pre-dose technique*. Radiat. Meas. **23**, 471–479 (1994).
7. Haskell, E. H. and Bailiff, I. K. *Diagnostic and corrective procedures for TL analysis using the predose technique*. Nucl. Tracks **10**, 503–508 (1985).
8. Haskell, E. H. and Bailiff, I. K. *TL dosimetry using bricks and tiles for measurement of transient gamma ray dose in inhabited areas*. Radiat. Prot. Dosim. **34**, 195–197 (1990).
9. Bailiff, I. K. and Haskell, E. H. *The use of the predose technique for environmental dosimetry*. Radiat. Prot. Dosim. **6**, 245–248 (1984).
10. Pagonis, V., Kitis, G. and Chen, R. *Applicability of the Zimmerman predose model in the thermoluminescence of predosed and annealed synthetic quartz samples*. Radiat. Meas. **37**, 267–274 (2003).
11. Bailiff, I. K. *Pre-dose dating: sensitization of R-traps?* Eur. PACT J. **9**, 207–214 (1983).
12. Aitken, M. J. *Pre-dose dating: predictions from the model*. Eur. PACT J. **9**, 319–324 (1979).